nature physics

LETTERS

PUBLISHED ONLINE: 24 MAY 2009 | DOI: 10.1038/NPHYS1284

Near-field electrical detection of optical plasmons and single-plasmon sources

Abram L. Falk[1]*, Frank H. L. Koppens[1]*, Chun L. Yu[2], Kibum Kang[3], Nathalie de Leon Snapp[2], Alexey V. Akimov[1], Moon-Ho Jo[3], Mikhail D. Lukin[1†] and Hongkun Park[1,2†]

Photonic circuits can be much faster than their electronic counterparts, but they are difficult to miniaturize below the optical wavelength scale. Nanoscale photonic circuits based on surface plasmon polaritons (SPPs) are a promising solution to this problem because they can localize light below the diffraction limit[1–8]. However, there is a general trade-off between the localization of an SPP and the efficiency with which it can be detected with conventional far-field optics. Here, we describe a new all-electrical SPP detection technique based on the near-field coupling between guided plasmons and a nanowire field-effect transistor. We use the technique to electrically detect the plasmon emission from an individual colloidal quantum dot coupled to an SPP waveguide. Our detectors are both nanoscale and highly efficient (~0.1 electrons per plasmon), and a plasmonic gating effect can be used to amplify the signal even higher (up to 50 electrons per plasmon). These results may enable new on-chip optical sensing applications and are a key step towards 'dark' optoplasmonic nanocircuits in which SPPs can be generated, manipulated and detected without involving far-field radiation.

Surface plasmon polaritons (SPPs) are charge-density waves that propagate along metal–dielectric interfaces. They can be concentrated and guided by current-carrying wires, suggesting an integrated approach to optical and electrical signal processing. Our near-field plasmon detection scheme consists of a Ag nanowire crossing a Ge nanowire field-effect transistor (Fig. 1, see the Methods section). The Ag nanowire guides[9] SPPs to the Ag–Ge junction, where they are converted to electron–hole pairs[10–12] and detected as current through the Ge nanowire.

The Ag nanowires are highly crystalline and defect-free[8,13,14], enabling SPPs to propagate over distances of several micrometres without scattering into free-space photons. Their narrow diameter (80–150 nm) supports tightly confined SPP modes, which couple weakly to the far-field but strongly to nearby Ge nanowire detectors and optical emitters. These characteristics enable us to demonstrate efficient, all-electrical detection of quantum-dot emission. The Ge nanowires also have narrow diameters (40–100 nm) and are highly sensitive to visible light[15], which makes our detection technique both efficient and spatially local.

Electrical plasmon detection is demonstrated by scanning a focused laser beam across a Ag–Ge crossbar device and recording the current (I) through the Ge nanowire as a function of the diffraction-limited laser spot position. These data, recorded at zero bias voltage (V_b), show that current flows through the Ge nanowire only when the laser beam is focused on four distinct spots on the device (Fig. 1b). First, current is detected when the laser is focused near the Ag–Ge junction, due to the direct photoresponse of the Ge nanowire[15]. The photocurrent signals induced on the left (I_{left}) and right (I_{right}) sides of the junction have opposite signs (discussed below). Moreover, current through the Ge nanowire (I_{plas}) is recorded when the laser is focused at either end of the Ag nanowire.

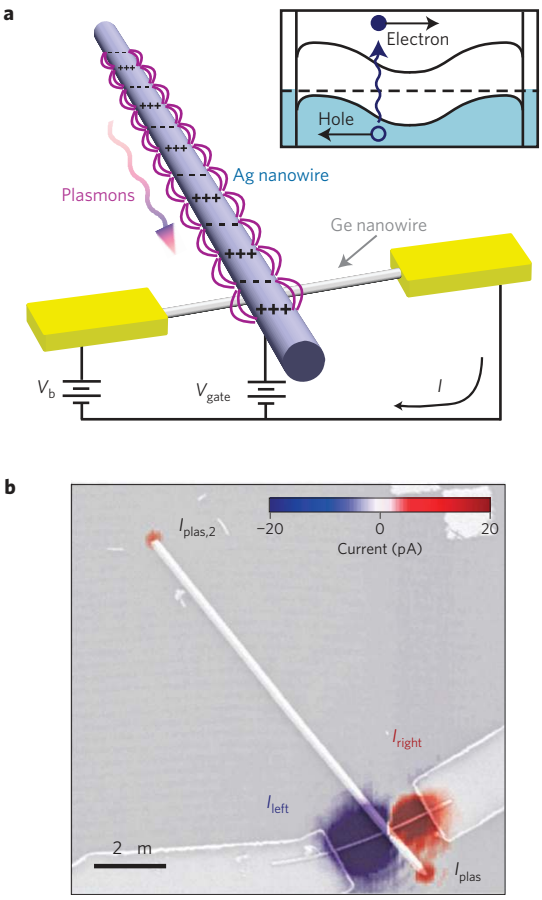

Figure 1 | Electrical plasmon detection. a, Schematic diagram of electrical plasmon detector operation. Inset: Electron–hole pair generation and separation in the Ge nanowire detector. **b**, Scanning electron micrograph of device 1, overlaid with the current through the Ge nanowire as a function of excitation laser position. Excitation laser power $P = 2.0\,\mu W$, wavelength $\lambda_{ex} = 532$ nm, $V_b = 0$, $V_{gate} = 0$.

[1]Department of Physics; [2]Department of Chemistry and Chemical Biology, Harvard University, 12 Oxford Street, Cambridge, Massachusetts 02138, USA, [3]Department of Materials Science and Engineering, Pohang University of Science and Technology, San 31, Hyoja-Dong, Nam-Gu, Pohang, Gyungbuk 790-784, Korea. *These authors contributed equally to this work. †e-mail: lukin@fas.harvard.edu; Hongkun_Park@harvard.edu.

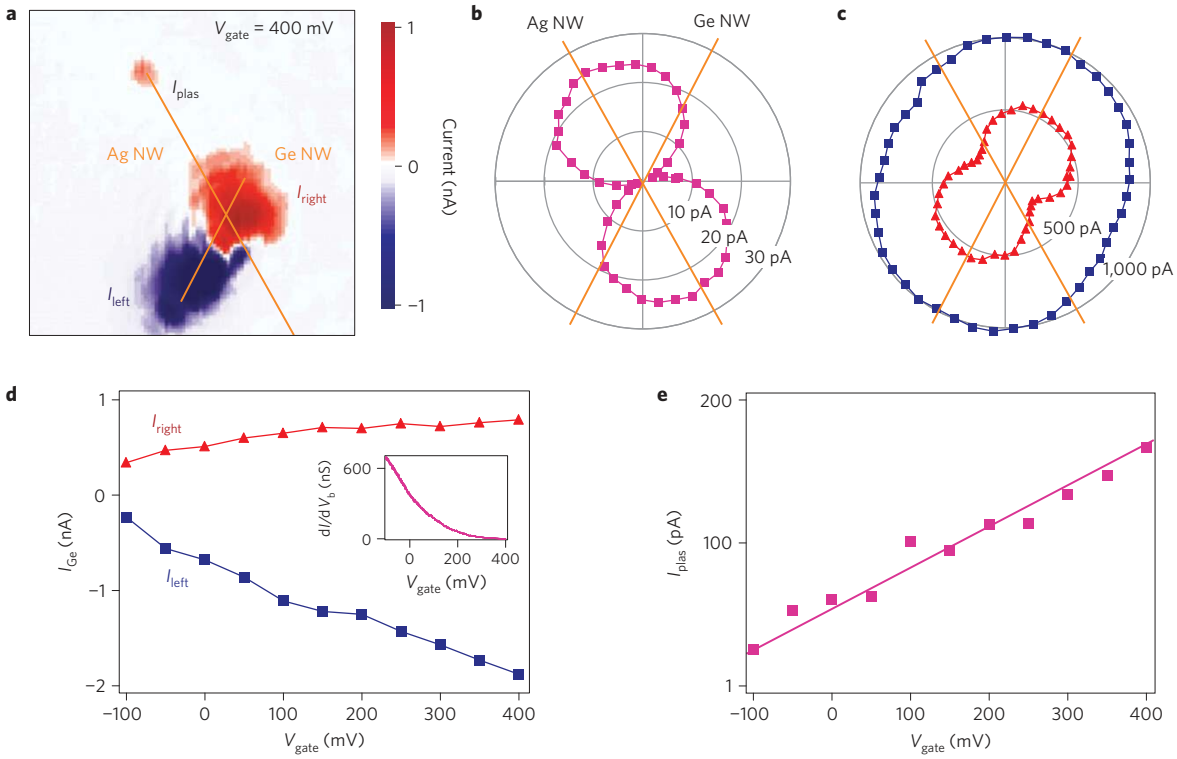

Figure 2 | Polarization and gate effects on plasmon detection. a, I as a function of laser spot position for device 2. $V_{gate} = 400$ mV, $V_b = 0$, $P = 3.4\,\mu$W, $\lambda_{ex} = 600$ nm. **b**,**c**, I_{plas} (**b**) and I_{right} (red triangles) and I_{left} (blue squares) (**c**) as a function of excitation light polarization. **d**, I_{right} (red triangles) and I_{left} (blue squares) as a function of V_{gate}. Inset: Gate response of the Ge nanowire conductance in nanosiemens. **e**, I_{plas} as a function of V_{gate}.

This I_{plas} signal is the key signature for electrical SPP detection. Propagating SPPs can be launched in the Ag nanowire only when the excitation laser is incident on the Ag nanowire ends[14]. Away from the ends, free-space photon-to-SPP conversion is strongly suppressed by the wave-vector mismatch between the two modes. If light scattered off the Ag nanowire were responsible for the current flowing through the Ge nanowire, signal would also be detected when the laser is focused on the middle of the Ag nanowire, in clear contrast to the data shown in Fig. 1b.

Further evidence for electrical SPP detection is provided by the dependence of I_{plas} on the polarization of the excitation laser. I_{plas} is largest when the excitation polarization is parallel to the Ag nanowire axis, and smallest when perpendicular (Fig. 2b). This preference reflects the conversion efficiency of the excitation light into SPP modes. The fundamental SPP mode consists of cylindrically symmetric charge oscillations along the Ag nanowire axis[16]. The excitation of this mode is suppressed when the excitation polarization is perpendicular to the wire axis. The direct Ge nanowire photocurrent is largest when the polarization axis is along the Ge nanowire (Fig. 2c), a consequence of the subwavelength nanowire diameter and the large dielectric contrast between the semiconductor and air[17].

An important figure of merit for our detector is the overall plasmon-to-charge conversion efficiency (η), defined as the ratio of detected charges to the number of SPPs reaching the Ag–Ge junction. The values of η in our devices typically ranged from 0.01 to 0.1 (see Supplementary Fig. S2). This efficiency can be tuned by applying a gate voltage (V_{gate}) to an extra electrical contact defined at one end of the Ag nanowire. In this geometry, the Ag nanowire is both the plasmon waveguide and a local electrical gate for the Ge nanowire (Fig. 2d, inset). As V_{gate} is increased, I_{plas} is enhanced (Fig. 2e), as are the magnitudes of I_{left} and I_{right} (Fig. 2d). Significantly, the magnitude of I_{plas} and thus η can be enhanced markedly by applying a non-zero bias to the Ge nanowire, increasing 300-fold as V_b is increased from 0 to 1 V (Fig. 3a). In some devices, η exceeded 50 electrons per plasmon at $V_b = 1$ V (Fig. 3b).

These results can be understood by considering electrical plasmon detection as a multistep process. First, the a.c. electric field of the SPP generates electron–hole pairs in the Ge nanowire through near-field coupling. Second, the d.c. electric field within the Ge nanowire separates these electron–hole pairs into free charges before recombination takes place. The separated electron–hole pairs are then detected as current. The shape of the built-in d.c. electric potential, a potential well (Fig. 1a, inset), can be inferred from the sign of the Ge photocurrent at either side of the Ag–Ge junction. The depth of this well is tuned by V_{gate} (ref. 15), explaining the monotonic dependence of I_{right}, I_{left} and I_{plas} on V_{gate} (Fig. 2d, e). Asymmetric electrical contacts to the Ge can cause the potential well in the Ge to be off-centre with respect to the Ag nanowire. This asymmetry explains the difference in magnitude of I_{right} and I_{left}, and determines the sign of the plasmon-induced current. The d.c. electric field in the Ge nanowire is non-zero even at $V_b = V_{gate} = 0$, owing to charge transfer across the Ag–Ge junction and/or the occupation of surface charge traps[15].

At $V_b = 0$, η is the genuine SPP detection efficiency. The amplification of this plasmon detection signal at non-zero V_b is due to a plasmon-induced gating effect, similar to the photogating effect observed previously in Ge nanowires[15]. When incident light or SPPs excite electron–hole pairs in the Ge nanowire, the minority carriers (electrons) have long lifetimes[18], especially when they can migrate to the nanowire surface and get trapped. These long-lived electrons attract free holes into the nanowire and increase the conductance, thereby producing electrical gain. The sublinear power dependence—η decreases as the excitation laser power increases (Fig. 3b)—reflects the saturation of surface charge traps on the Ge nanowire.

Finite-difference time-domain (FDTD) simulations of our devices provide further insight into the device operation. In these

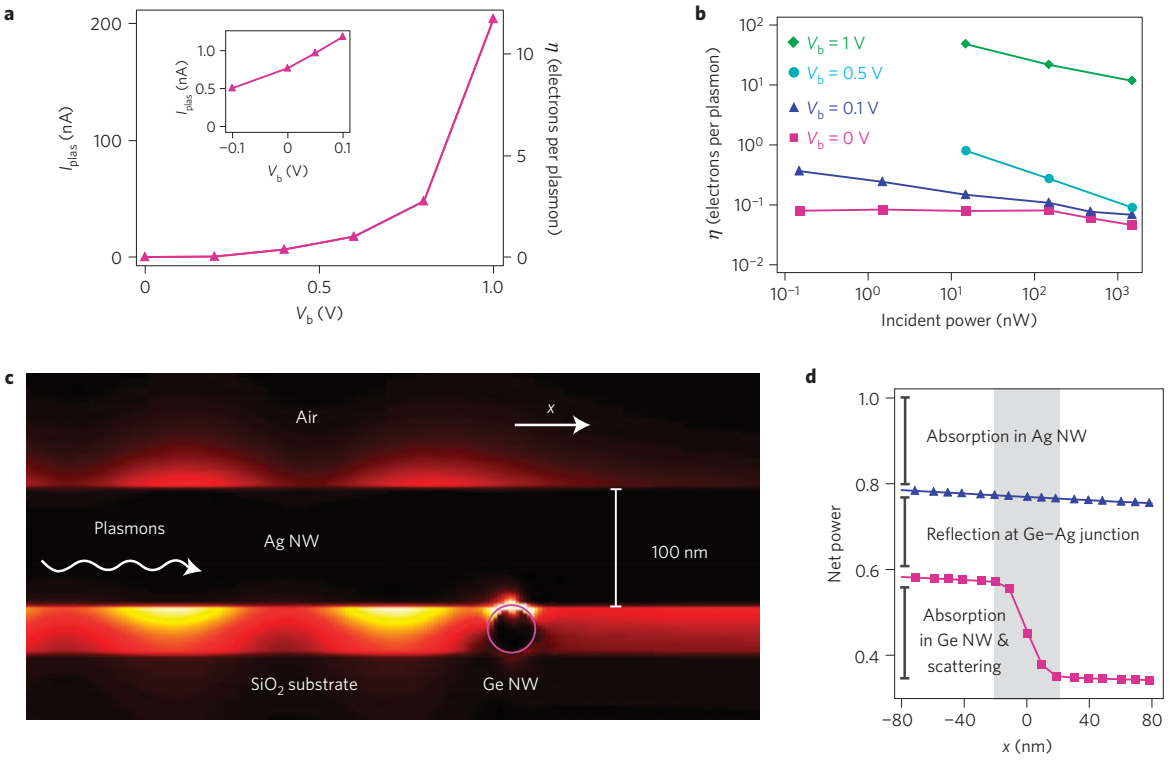

Figure 3 | Gain in plasmon detectors and simulation. a, I_{plas} as a function of V_b for device 3. $P = 1.5\,\mu W$, $V_{gate} = 0$, $\lambda_{ex} = 600$ nm, Ag nanowire diameter = 100 nm, Ge nanowire diameter = 40 nm. Inset: I_{plas} as a function of V_b for smaller values of V_b. **b**, η as a function of P and V_b. **c**, FDTD simulation of electric-field intensity. Ag nanowire diameter = 100 nm, Ge nanowire diameter = 40 nm. **d**, Net power in the plasmon mode as a function of distance (x) along the Ag nanowire from the Ge nanowire centre. At $x = 0$, the net power drops in the Ag–Ge device (violet squares) owing to absorption in the Ge nanowire and scattering, whereas there is no sudden drop in a simple Ag nanowire with no Ge crossbar (blue triangles). The shaded area represents the position of the Ge nanowire. Approximately 30% of the SPP energy is reflected, 3% scatters to the far-field, 20% is absorbed by the Ge nanowire and the rest is transmitted.

simulations, an SPP pulse is launched in the fundamental mode of the Ag nanowire. As it propagates, the electric field intensity (Fig. 3c) and Poynting vector (Fig. 3d) are monitored as functions of position and time. Once the SPP flux reaches the Ge–Ag junction, it can be reflected, transmitted, absorbed by the Ge nanowire or scattered to the far-field. The simulation results show that a 40-nm-diameter Ge nanowire absorbs 20 (50)% of the SPP flux when the Ag nanowire diameter is 100 (50) nm (Fig. 3d and Supplementary Fig. S3). This large absorption fraction originates from the high absorption constant[19] of Ge and the strong SPP confinement, which increases for smaller Ag nanowire diameters.

A comparison of the simulated Ge absorption fraction (20%) and the experimentally measured η values (1–10% at $V_b = 0$) suggests that SPP absorption by the Ge nanowire is not the main factor that limits our detectors' efficiencies. We note that an electric-field profile that is perfectly symmetric with respect to the Ag nanowire axis would not result in a net current flow at $V_b = 0$ when cylindrically symmetric SPPs impinge on the Ag–Ge junction. As such, the sign and magnitude of I_{plas} reflect the contact asymmetry at the Ag–Ge junction, and properly designed asymmetric gates could enhance the intrinsic efficiency.

We demonstrate the utility of our near-field SPP detector by electrically detecting emission from a CdSe quantum dot acting as a single-plasmon source (Fig. 4). The tight field confinement around Ag nanowires causes a large fraction of the spontaneous emission from nearby emitters (30–100 nm away) to be captured as SPP modes[20–22]. These SPPs are then converted into an electrical signal at a Ge nanowire detector. Individual quantum dots are coupled to a Ag nanowire by covering a Ag–Ge device with a 30 nm film of poly(methyl methacrylate) containing a dilute concentration of chemically synthesized CdSe quantum dots. Optical fluorescence measurements (Fig. 4a) show that some quantum dots are close to the Ag nanowire. When the laser excites one of these quantum dots, a current signal in the Ge nanowire detector is observed (I_1, circled in Fig. 4b) in addition to optical fluorescence from the quantum dot.

The dependence of this signal on the excitation wavelength (λ_{ex}) is clear proof that the current signal results from quantum-dot emission (Fig. 4c). This spectrum, a downward trend with increasing λ_{ex} and a distinct peak at 655 nm, closely resembles the absorption spectrum of CdSe quantum dots[23]. In contrast, when plasmons are launched from a nanowire end by direct photon-to-SPP conversion (I_2, circled in Fig. 4b), the spectrum exhibits a gradual upward trend with increasing λ_{ex}, as expected from the longer SPP propagation lengths at higher wavelengths[1]. Significantly, photon correlation measurements of the far-field fluorescence (Fig. 4d) demonstrate a clear anti-bunching signature, indicating that this spot corresponds to an individual quantum dot. Finally, the detector does not record a current above the noise level (root mean square 0.1 pA) when the laser is focused on quantum dots that are away from the Ag nanowire, such as the one circled in green in Fig. 4a, b. Taken together, these measurements prove that single quantum-dot emission captured into SPPs can be detected electrically without intermediate far-field photons (see Supplementary Information S4 for a discussion of the sign of I_1 and I_2 and an extra quantum-dot detection data set).

When the quantum dots are excited at $\lambda_{ex} = 500$ nm, we find $I_{plas} \sim 1$ pA at $V_b = 0$, corresponding to $\sim 6 \times 10^6$ electrons s^{-1}. Assuming that the quantum-dot emission directed into plasmons

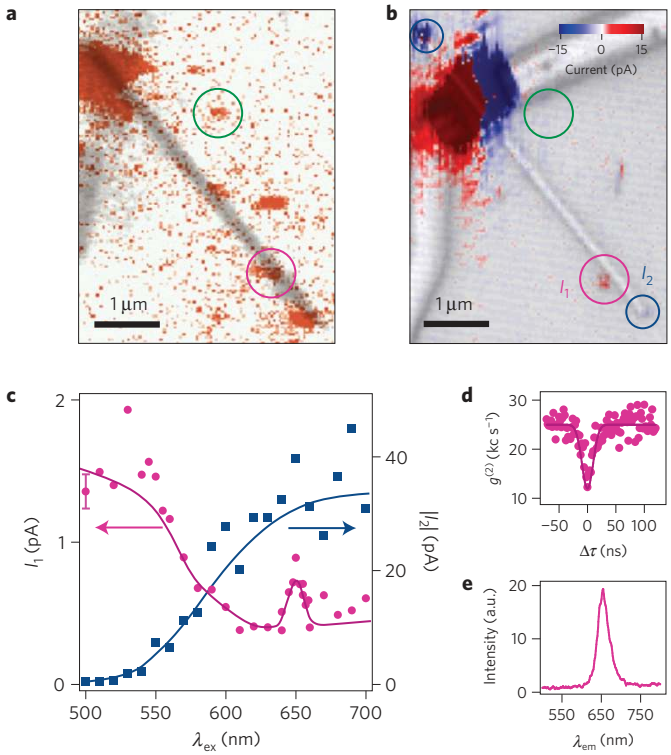

Figure 4 | Electrical detection of emission from a single CdSe colloidal quantum dot. a, Optical emission from quantum dots, measured with a confocal microscope, overlayed on a reflection image. The emission is filtered with a 600 nm long-pass filter. **b**, I as a function of laser position, overlaying a reflection image of device 4. $P = 1.5\,\mu W$, $\lambda_{ex} = 530$ nm. $V_b = 0$, $V_{gate} = 0$. The violet circle indicates the detector signal corresponding to quantum-dot emission into the Ag nanowire plasmon modes. The blue circles correspond to detection of surface plasmons launched directly by the laser, at the ends of the nanowire. The green circle corresponds to the position of a quantum dot that is not near the Ag nanowire, and hence does not generate a current in the detector. **c**, I_1 (quantum-dot emission, violet circles) and I_2 (direct laser-to-plasmon signal, blue squares) as a function of λ_{ex}. **d**, Second-order self-correlation function $g^{(2)}(\tau)$ of the quantum-dot fluorescence. The coincidence rate at $\tau = 0$ approaches 0.5, confirming that a single quantum dot is present. **e**, Quantum-dot emission spectrum.

equals its far-field emission, a typical quantum dot can generate up to 5×10^7 plasmons s^{-1} (ref. 20). This simple consideration implies that the detection efficiency of the quantum-dot emission is ~0.1 electronsper plasmon, consistent with the η value of this device at $V_b = 0$ (see Supplementary Fig. S2).

Nanoscale near-field SPP detection opens up several directions for further research. An electrical SPP detector could be mounted on a scanning tip, providing a new SPP imaging technique. In conjunction with an electrically driven plasmon source[24], a near-field SPP detector could be integrated into a 'dark' optoelectronic–plasmonic nanocircuit in which all coupling is in the near-field. The plasmon-detection sensitivity could be improved by using a nanoscale avalanche photodiode[25] as the SPP detector, potentially enabling efficient electrical detection of individual plasmons. Electrical plasmon detectors could lead to new applications for optical sensing without collection optics, including the measurement of plasmon states in which coupling to the far-field is suppressed by symmetry[26]. Finally, the strong near-field coupling between single-plasmon emitters and plasmonic nanocircuits could lead to completely new capabilities that are not available with conventional photonics, such as nonlinear switches, single-photon transistors and quantum non-demolition detectors[21,27,28].

Methods

The Ag nanowires used in our experiments were synthesized using a modified polyol method described previously[13]. The Ge nanowires were synthesized using a vapour–liquid–solid chemical vapour deposition technique[29,30]. They were catalysed by Au nanoparticles, grown in GeH_4/H_2 gas and subsequently doped to be p-type in B_2H_4/H_2 gas.

The SPP detectors were fabricated by drop-casting Ge nanowires and Ag nanowires on a degenerately doped Si substrate with 300 nm SiO_2 grown on top. Once the Ag–Ge nanowire crossbars were identified, the Ge nanowires were electrically contacted using conventional electron beam lithography and Ti/Au metal deposition (15 nm/150 nm).

The excitation of SPPs was carried out using a Koheras SuperK supercontinuum laser. The laser was coupled to an acousto-optic tunable filter, enabling the excitation wavelength to be selected. The beam was spatially filtered through a pinhole, and then directed to an optical microscope using a scanning mirror. The objective lens of the microscope (×100, 0.8 numerical aperture) focused the beam to a diffraction-limited spot on the device. The details of the photon correlation measurement used for measuring the quantum-dot emission statistics are given elsewhere[20].

Received 20 January 2009; accepted 22 April 2009; published online 24 May 2009

References

1. Barnes, W. L., Dereux, A. & Ebbesen, T. W. Surface plasmon subwavelength optics. *Nature* **424**, 824–830 (2003).
2. Haes, A. J. & Van Duyne, R. P. A unified view of propagating and localized surface plasmon resonance. *Anal. Bioanal. Chem.* **379**, 920–930 (2004).
3. Ozbay, E. Plasmonics: Merging photonics and electronics at nanoscale dimensions. *Science* **311**, 189–193 (2006).
4. Atwater, H. A., Maier, S., Polman, A., Dionne, J. A. & Sweatlock, L. The new p–n junction: Plasmonics enables photonic access to the nanoworld. *MRS Bull.* **30**, 385–389 (2005).
5. Engheta, N. Circuits with light at nanoscales: Optical nanocircuits inspired by metamaterials. *Science* **1**, 1698–1702 (2007).
6. Pacifici, D., Lezec, H. J. & Atwater, H. A. All-optical modulation by plasmonic excitation of CdSe quantum dots. *Nature Photon.* **1**, 402–406 (2007).
7. Bozhevolnyi, S. I., Volkov, V. S., Devaux, E., Laluet, J. Y. & Ebbesen, T. W. Channel plasmon subwavelength waveguide components including interferometers and ring resonators. *Nature* **440**, 508–511 (2006).
8. Ditlbacher, H. *et al.* Silver nanowires as surface plasmon resonators. *Phys. Rev. Lett.* **95**, 257403 (2005).
9. Dickson, R. M. & Lyon, L. A. Unidirectional plasmon propagation in metallic nanowires. *P. Phys. Chem. B.* **104**, 6095–6098 (2000).
10. De Vlaminck, I., Van Dorpe, P., Lagae, L. & Borghs, G. Local electrical detection of single nanoparticle plasmon resonance. *Nano Lett.* **7**, 703–706 (2007).
11. Mapel, J. K., Singh, M., Baldo, M. A. & Celebi, K. Plasmonic excitation of organic double heterostructure solar cells. *Appl. Phys. Lett.* **90**, 121102 (2007).
12. Ditlbacher, H. *et al.* Organic diodes as monolithically integrated surface plasmon polariton detectors. *Appl. Phys. Lett.* **89**, 161101 (2006).
13. Wiley, B., Sun, Y. & Xia, Y. Polyol synthesis of silver nanostructures. *Langmuir* **21**, 8077–8080 (2005).
14. Sanders, A. W. *et al.* Observation of plasmon propagation, redirection, and fan-out in silver nanowires. *Nano Lett.* **6**, 1822–1826 (2006).
15. Ahn, Y. & Park, J. Efficient visible light detection using individual germanium nanowire field effect transistors. *Appl. Phys. Lett.* **91**, 162102 (2007).
16. Takahara, J., Yamagishi, S., Taki, H., Morimoto, A. & Kobayashi, T. Guiding of a one-dimensional optical beam with nanometer diameter. *Opt. Lett.* **22**, 475–477 (1997).
17. Wang, J., Gudiksen, M. S., Duan, X., Cui, Y. & Lieber, C. M. Highly polarized photoluminescence and photodetection from single indium phosphide nanowires. *Science* **293**, 1455–1457 (2001).
18. Razeghi, M. & Rogalski, A. Semiconductor ultraviolet detectors. *J. Appl. Phys.* **79**, 7433–7473 (1996).
19. Palik, E. D. *Handbook of Optical Contents of Solids III* (Academic, 1997).
20. Akimov, A. V. *et al.* Generation of single optical plasmons in metallic nanowires coupled to quantum dots. *Nature* **450**, 402–406 (2007).
21. Chang, D. E., Sorenson, A. S., Hemmer, P. R. & Lukin, M. D. Strong coupling of single emitters to surface plasmons. *Phys. Rev. B* **76**, 035420 (2007).
22. Chang, D. E., Sorenson, A. S., Hemmer, P. R. & Lukin, M. D. Quantum optics with surface plasmons. *Phys. Rev. Lett.* **97**, 053002 (2006).
23. Brus, L. Zero-dimensional 'excitons' in semiconductor clusters. *IEEE J. Quantum Electron.* **22**, 1909–1914 (1986).
24. Koller, D. M. *et al.* Surface plasmon coupled electroluminescent emission. *Appl. Phys. Lett.* **92**, 103304 (2008).
25. Hayden, O., Agarwal, R. & Lieber, C. M. Nanoscale avalanche photodiodes for highly sensitive and spatially resolved photon detection. *Nature Mater.* **5**, 352–356 (2006).

26. Nordlander, P., Oubre, C., Prodan, E., Li, K. & Stockman, M. I. Plasmon hybridization in nanoparticle dimers. *Nano Lett.* **4**, 899–904 (2004).
27. Chang, D. E., Sorensen, A. S., Demler, E. A. & Lukin, M. D. A single-photon transistor using nanoscale surface plasmons. *Nature Phys.* **3**, 807–812 (2007).
28. Smolyaninov, I. I., Zayats, A. V., Gungor, A. & Davis, C. C. Single-photon tunneling via localized surface plasmons. *Phys. Rev. Lett.* **88**, 187402 (2002).
29. Greytak, A. B., Lauhon, L. J., Gudksen, M. S. & Lieber, C. M. Growth and transport properties of complementary germanium nanowire field-effect transistors. *Appl. Phys. Lett.* **84**, 4176–4178 (2004).
30. Yang, J. E., Jin, C. B., Kim, C. J. & Jo, M. H. Band-gap modulation in single-crystalline $Si_{1-x}Ge_x$ nanowires. *Nano Lett.* **6**, 2679–2684 (2006).

Acknowledgements

We would like to acknowledge D. Chang, G. Abstreiter and M. Stutzmann for valuable discussions and M. McCutcheon for assistance with the FDTD simulations. This work was supported by the Defense Advanced Research Projects Agency, the National Science Foundation, the Air Force Office of Scientific Research and Samsung Electronics.

Author contributions

A.F. and F.K. carried out the measurements. A.F., F.K., M.L. and H.P. analysed the data and wrote the manuscript. H.P. and M.L. supervised the project. C.Y., K.K. and M.J. synthesized the nanostructures. N.S. and A.A. helped build the experimental apparatus. All of the authors discussed the results and manuscript extensively.

Additional information

Supplementary information accompanies this paper on www.nature.com/naturephysics. Reprints and permissions information is available online at http://npg.nature.com/reprintsandpermissions. Correspondence and requests for materials should be addressed to M.D.L. or H.P.